Heteroleptic arene Ru(II) dipyrrinato complexes: DNA, protein binding and anti-cancer activity against ACHN cancer cell line

Rakesh Kumar Gupta,[a] Amit Kumar,[a] Rajendra Prasad Paitandi,[a] Roop Shikha Singh,[a] Sujay Mukhopadhyay,[a] Shiv Prakash Verma,[b] Parimal Das[b] and Daya Shankar Pandey*[a]

[a]Department of Chemistry, Institute of Science, Banaras Hindu University, Varanasi - 221 005 (U.P.) India

[b]Centre for Genetic Disorders, Banaras Hindu University, Varanasi - 221 005 (U.P.) India

Contents

1. NMR spectra of the ligands and complexes **1**–**4**……S2-S7

2. HOMO LUMO diagram of complexes **1**–**4**……S8-S9

3. Absorption titration spectra of **1**, **2** and **4** with CT DNA……S10

4. Emission spectra from EB bound to DNA with **1**, **2** and **4**……S11

5. Emission spectra of BSA with **1**, **2** and **4**……S12

6. Stern-Volmer plot for complexes at different temperature……S13

7. Synchronous spectra of BSA with **1**, **2** and **4** at $\Delta\lambda$ = 60 nm……S14

8. Synchronous spectra of BSA with **1**, **2** and **4** at $\Delta\lambda$ = 15 nm……S15

9. 3D fluorescence spectra of BSA with **1**, **2** and **4**……S16

10. HRMS spectra of ligand and **1**–**4**……S17-S19

11. Molecular docking of **1**, **2** and **4** with DNA and Protein……S20-S25

12. Anti-proliferative profiles of **1**–**4**……S26

13. Selected bond lengths and bond angles (˚) from DFT calculation……S27

14. HOMO LUMO energy of complexes **1**–**4**……S27

15. Absorption Spectral data of **1**–**4** bound to CT DNA……S28

16. Quenching constant and binding constant (K_{bin}) of **1**–**4** with BSA……S29

17. 3D fluorescence spectral parameters of the BSA and BSA + **1**–**4**……S30

18. Log *P* Values for Complexes **1**–**4**……S31

19. Binding site of protein (HSA)……S32-S33

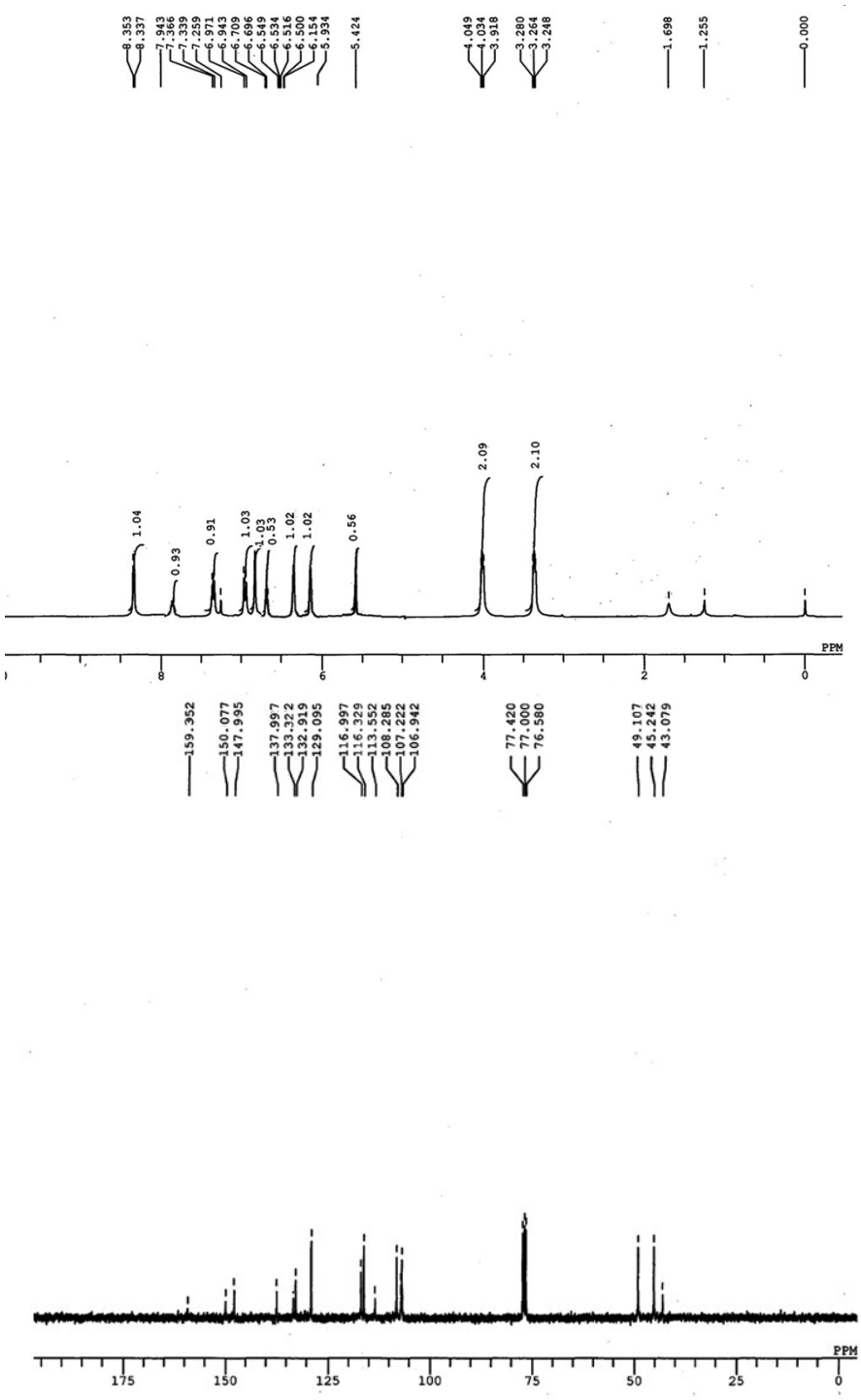

Fig. S1 ^{1}H (top) and ^{13}C NMR (bottom) spectra of **pmpzdpmH** in $CDCl_3$.

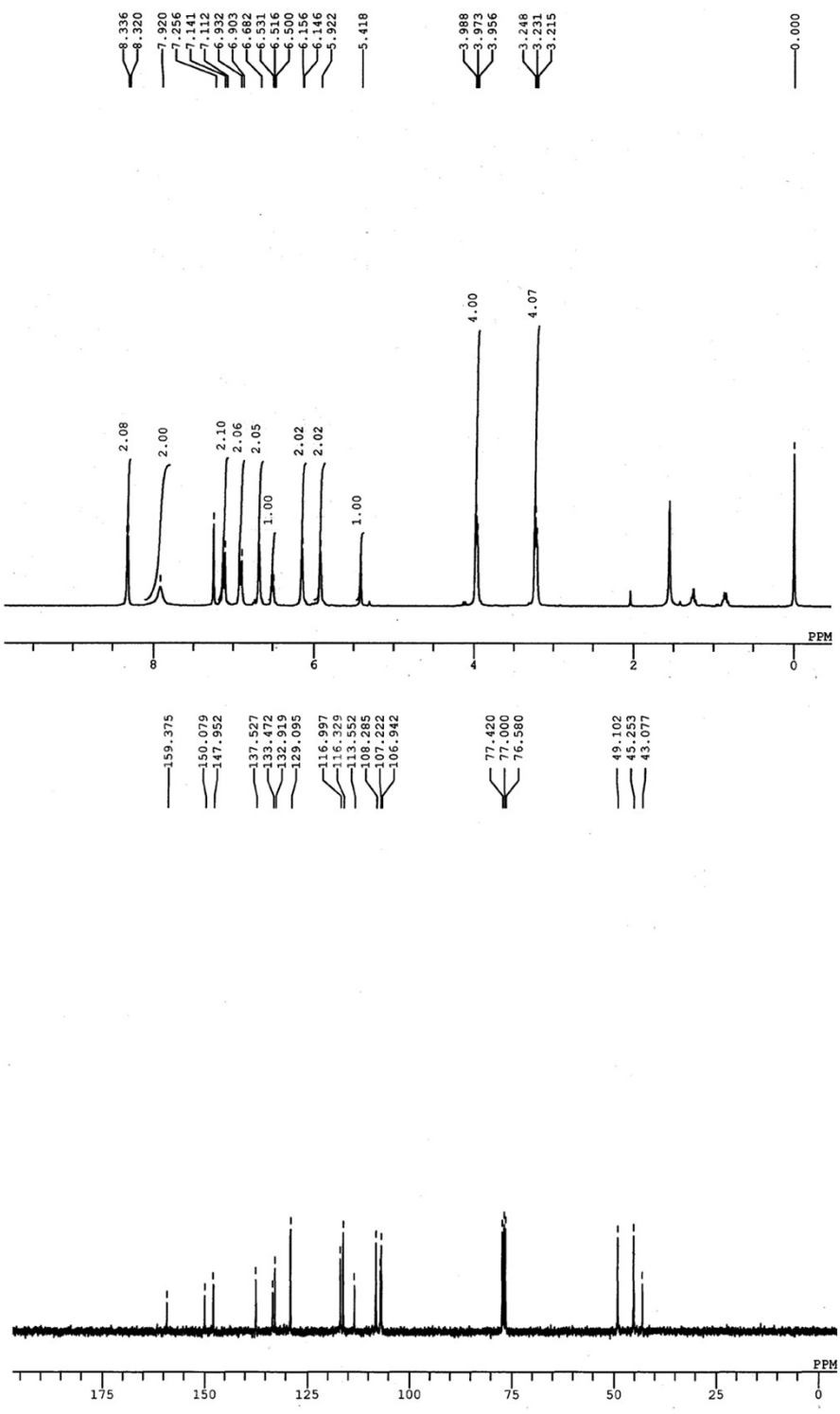

Fig. S2 ^{1}H (top) and ^{13}C NMR (bottom) spectra of **pypzdpmH** in $CDCl_3$.

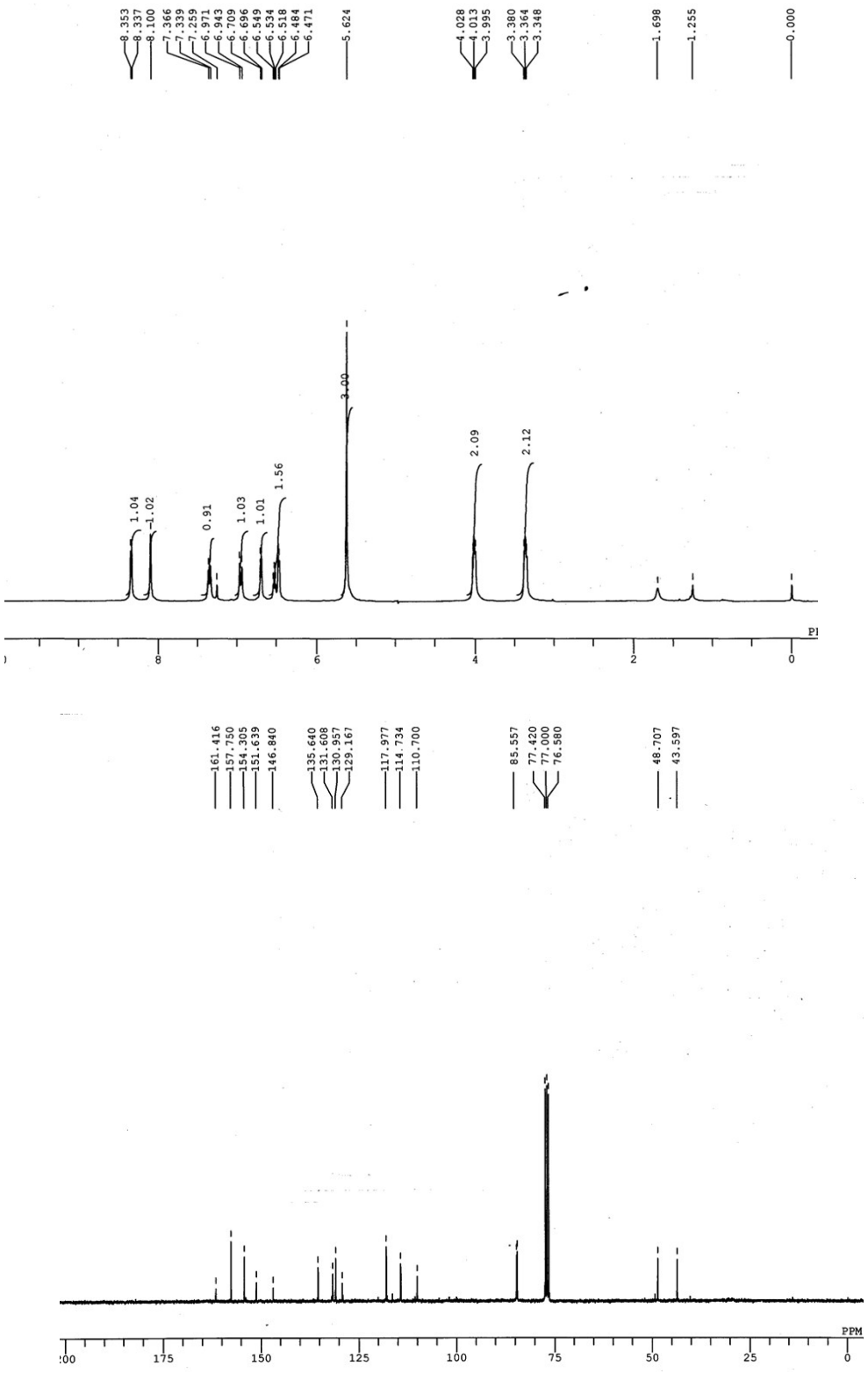

Fig. S3 ^{1}H (top) and ^{13}C NMR (bottom) spectra of **1** in $CDCl_3$.

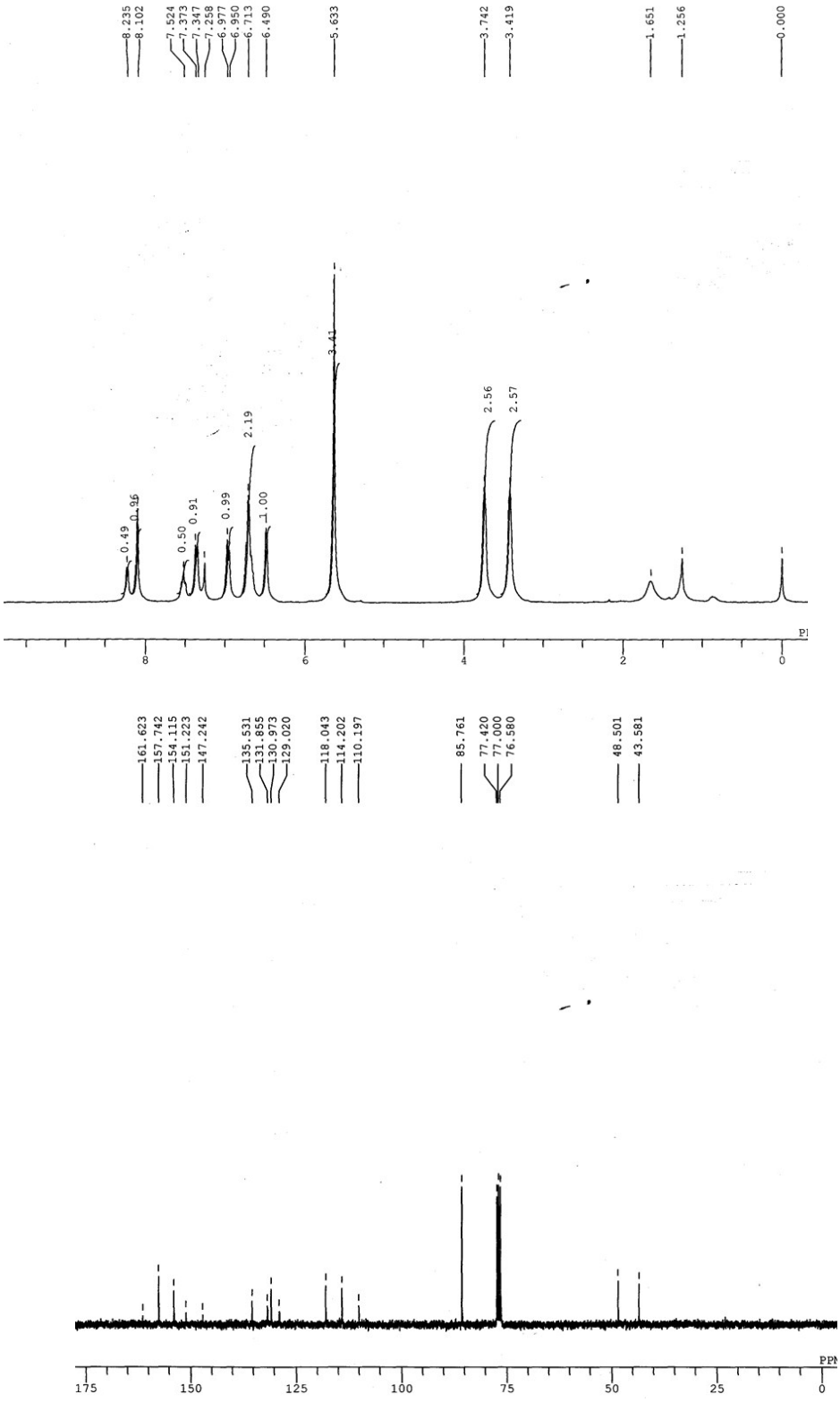

Fig. S4 ^{1}H (top) and ^{13}C NMR (bottom) spectra of **2** in $CDCl_3$.

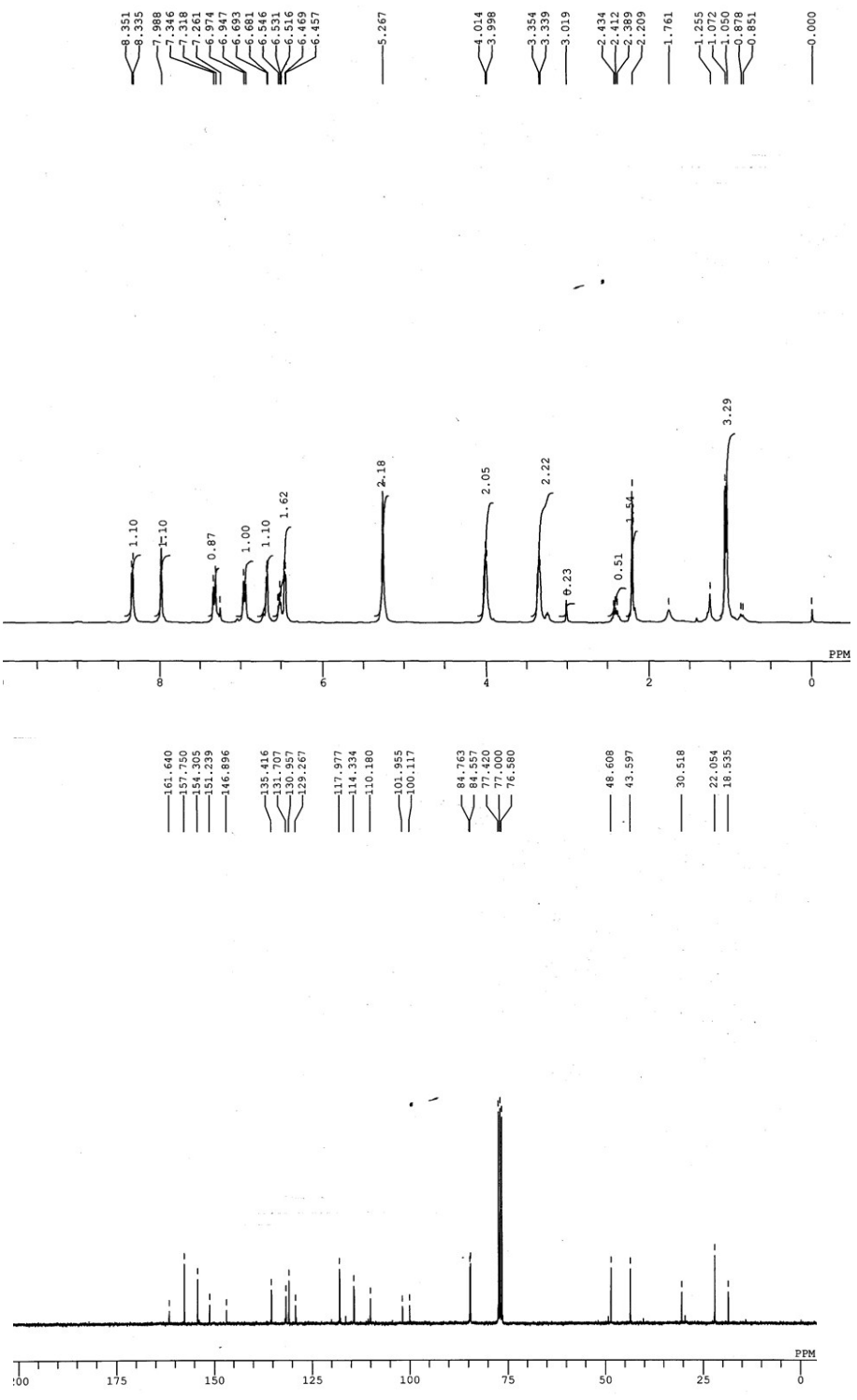

Fig. S5 ^{1}H (top) and ^{13}C NMR (bottom) spectra of **3** in $CDCl_3$.

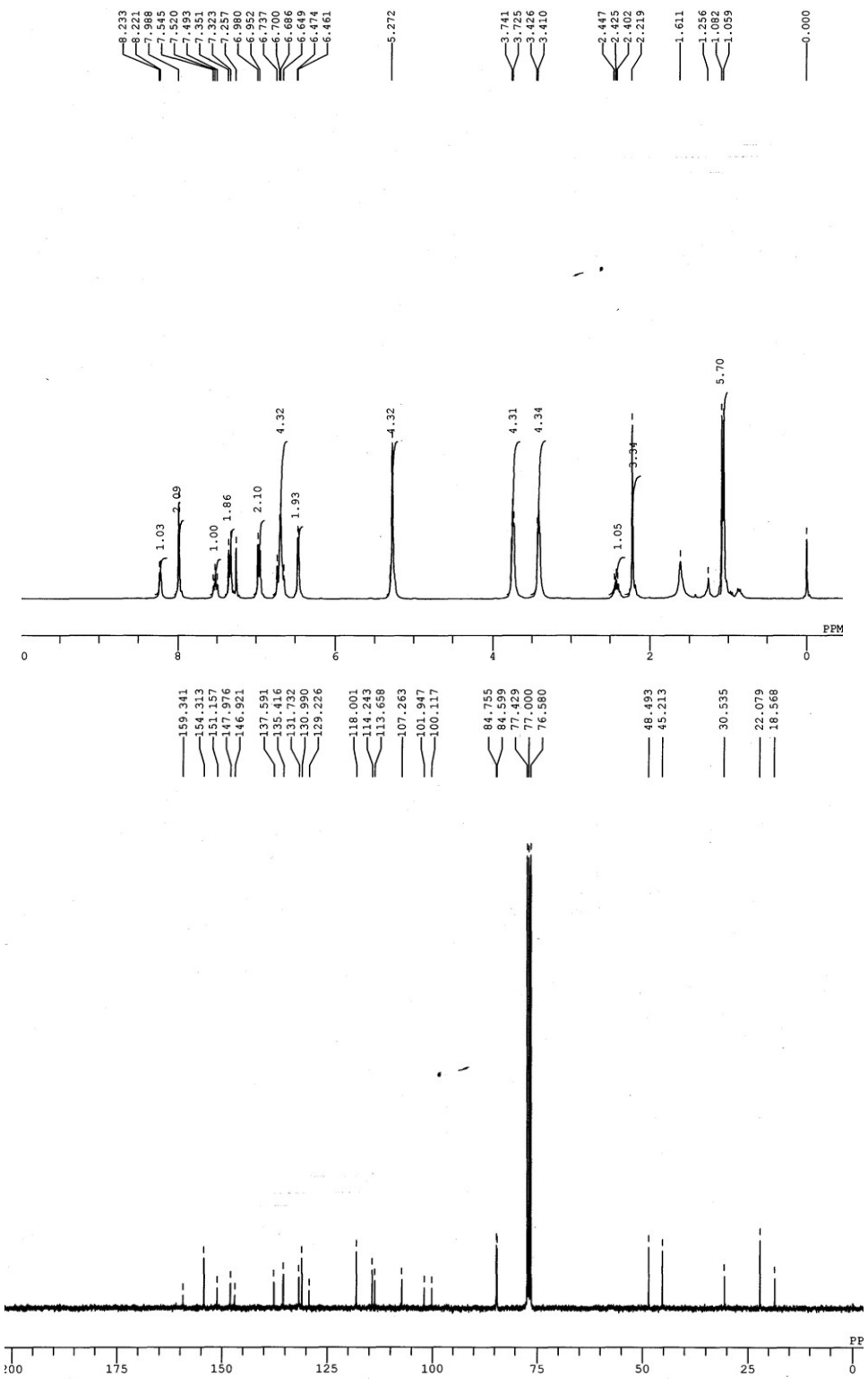

Fig. S6 ^{1}H (top) and ^{13}C NMR (bottom) spectra of **4** in $CDCl_3$.

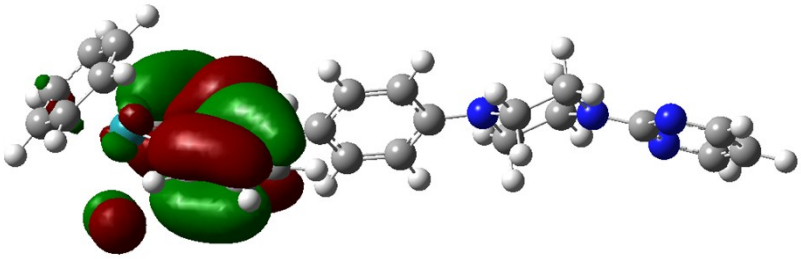

(a)

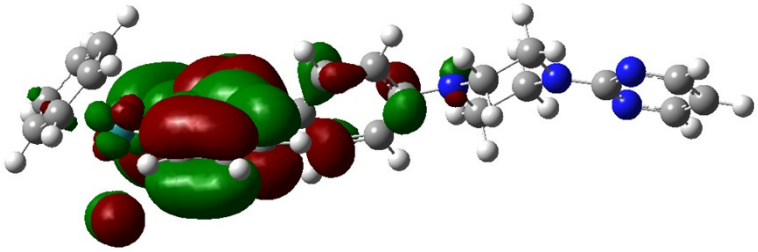

(b)

Fig. S7 HOMO (a) LUMO (b) diagram of complex **1**.

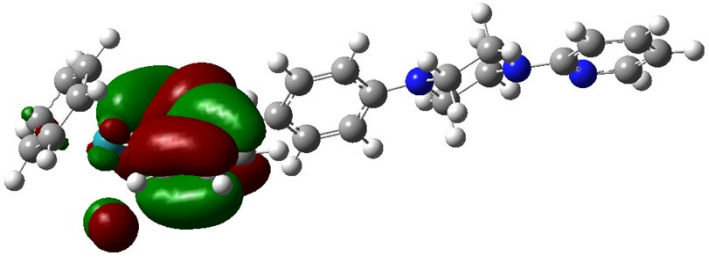

(a)

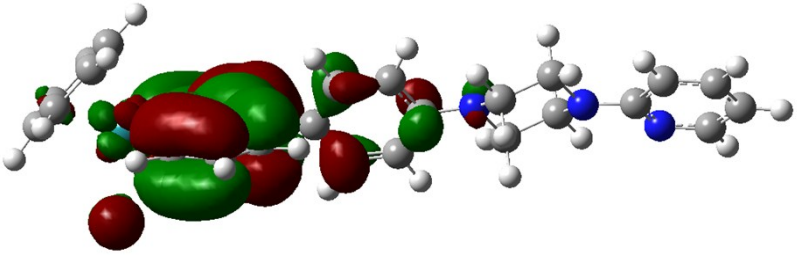

(b)

Fig. S8 HOMO (a) LUMO (b) diagram of complex **2**.

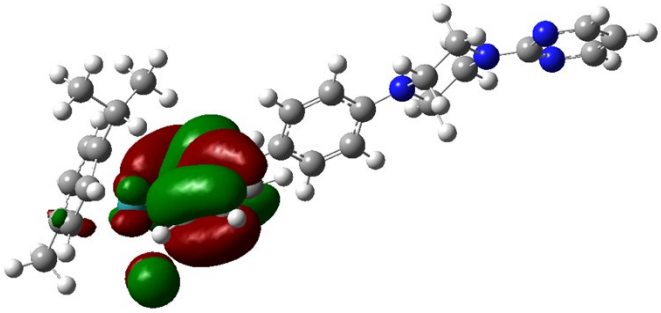

(a)

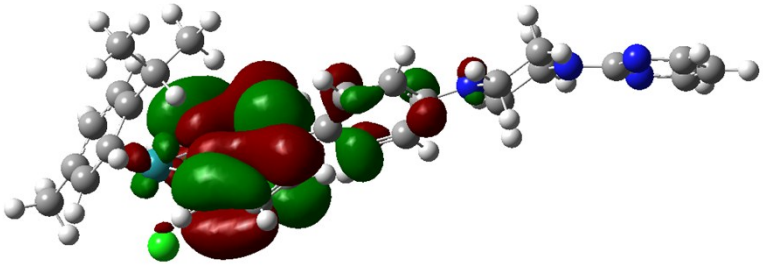

(b)

Fig. S9 HOMO (a) LUMO (b) diagram of complex **3**.

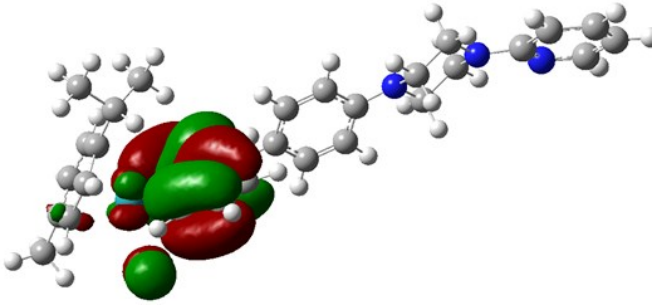

(a)

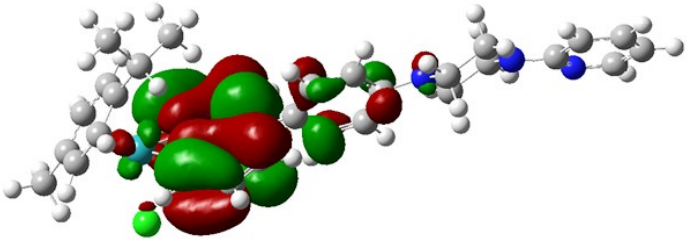

(b)

Fig. S10 HOMO (a) LUMO (b) diagram of complex **4**.

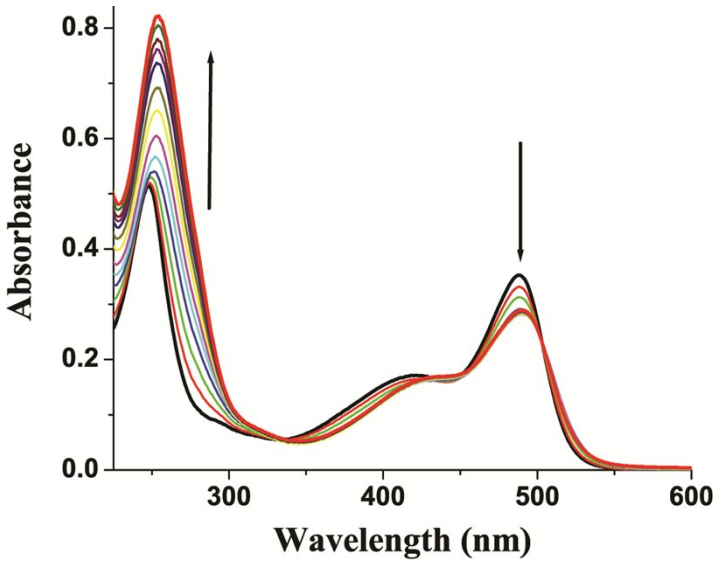

(a)

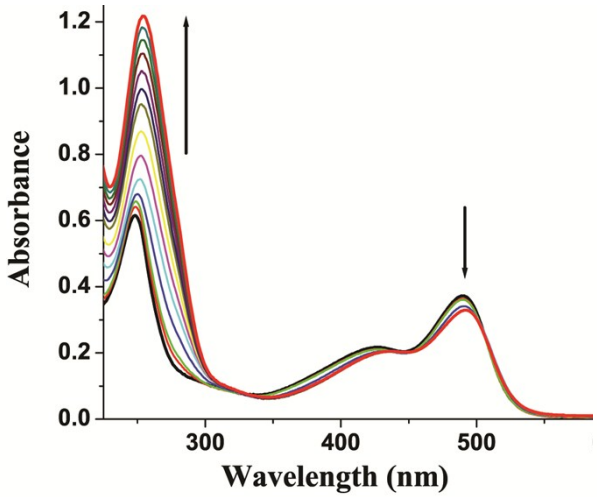

(b)

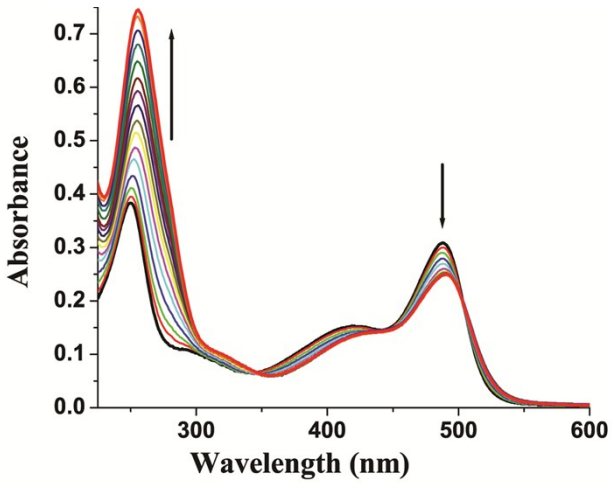

(c)

Fig. S11 Absorption titration spectra of **1** (a), **2** (b) and **4** (d) in EtOH:H_2O (1:1) with an increase in molar ratio of CT DNA to complex (1–30 μM) at rt. Arrow shows the absorbance changes upon increasing CT DNA concentration.

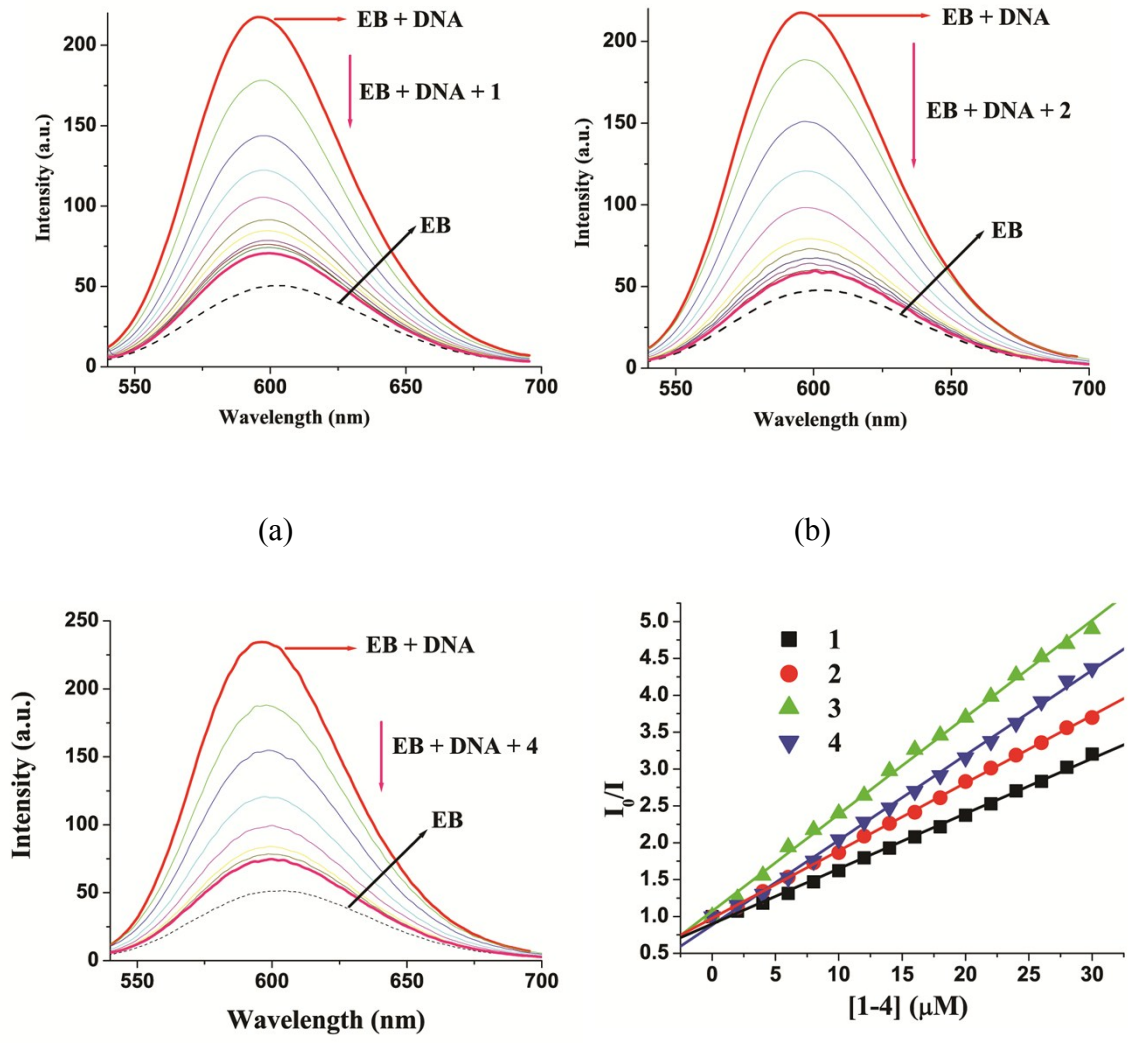

Fig. S12 Emission spectra of EB bound to the DNA in the absence (---) and in the presence of **1** (a), **2** (b) and **4** (c). [EB] = 10 μM, [DNA] = 10 μM, [**1**, **2** and **4**] = 0–50 μM. Arrow shows changes in the emission intensity upon addition of increasing complex concentration. Stern−Volmer plots of the EtBr-DNA fluorescence titration for complexes **1**−**4** (d).

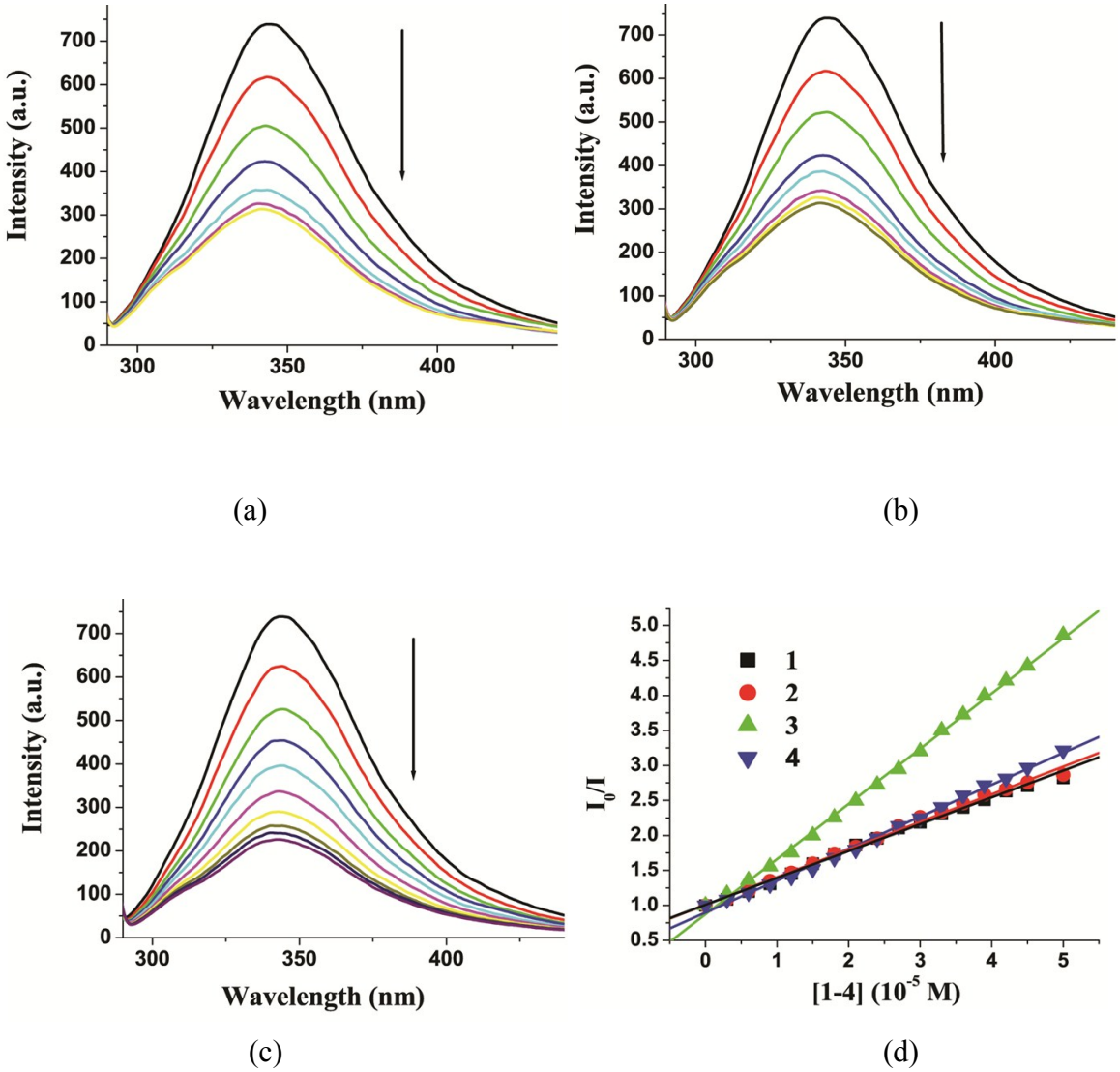

Fig. S13 Emission spectrum of BSA (0.5 μM; λ_{ex} = 280 nm; λ_{em} = 343 nm) in the presence of increasing amounts of complexes **1** (a), **2** (b) and **4** (c) (0–50 μM). Stern−Volmer plots of the fluorescence titrations of **1**−**4** (d).

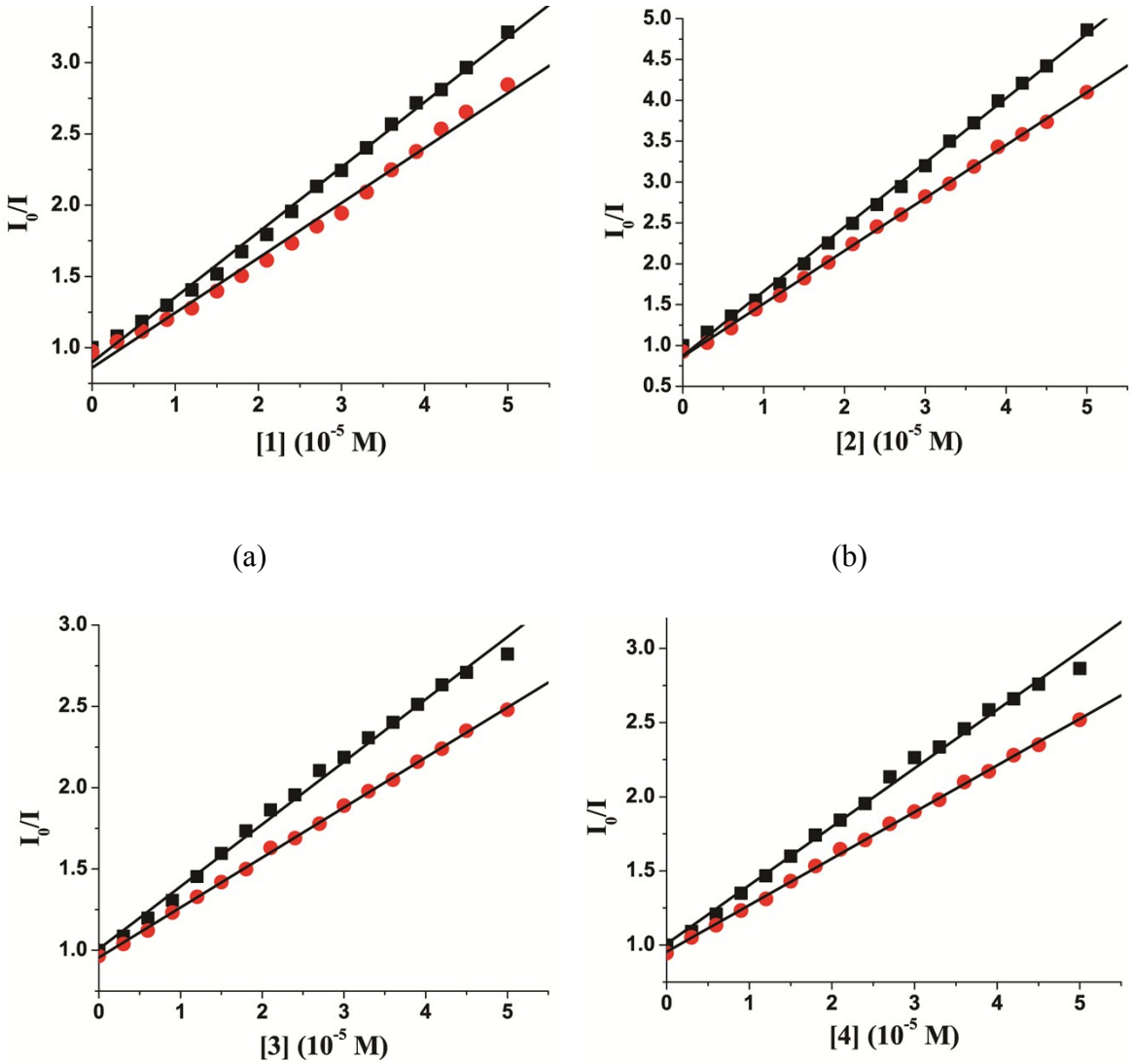

Fig. S14 Stern-Volmer plot for quenching of complexes **1** (a), **2** (b), **3** (c) and **4** (d) to BSA at 300 (black) and 310 K (red).

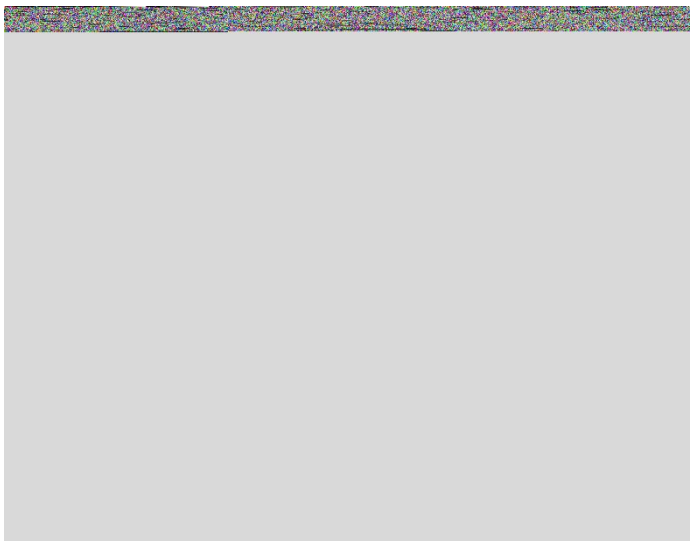

(a)

(b) (c)

Fig. S15 Synchronous spectra of BSA (0.5 μM) in the presence of increasing amounts of complexes **1** (a), **2** (b) and **4** (c) (0–50 μM) in the wavelength difference of $\Delta\lambda$ = 60 nm. Arrows show the emission intensity decrease accompanied by blue shift upon the increasing concentration of complexes **1**, **2** and **4**.

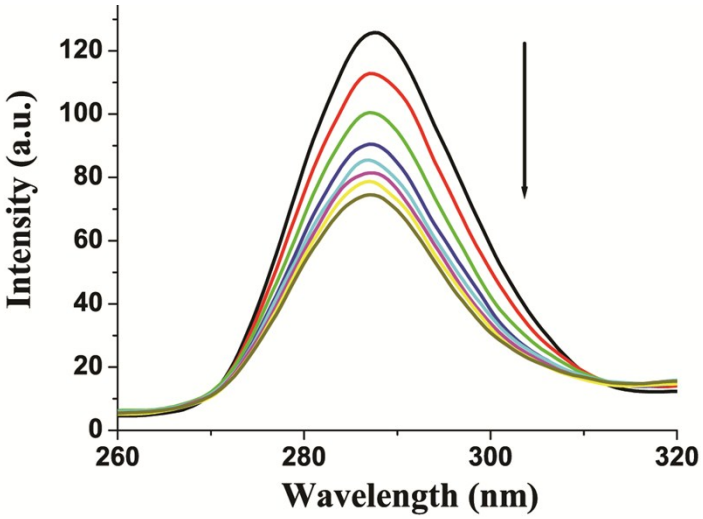

(a)

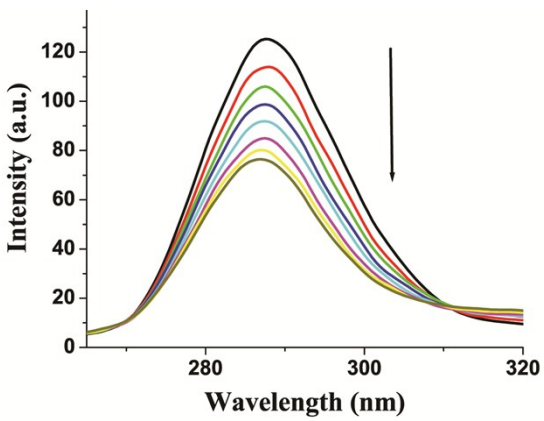

(b)

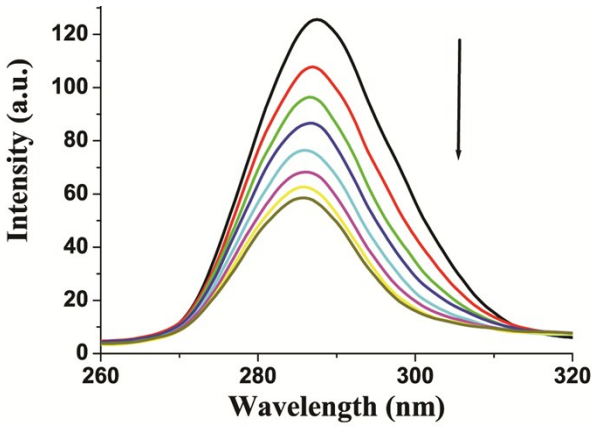

(c)

Fig. S16 Synchronous spectra of BSA (0.5 μM) in the presence of increasing amounts of complexes **1** (a), **2** (b) and **4** (c) (0–50 μM) in the wavelength difference of $\Delta\lambda$ = 15 nm. Arrows show the emission intensity decrease accompanied by blue shift upon the increasing concentration of complexes **1**, **2** and **4**.

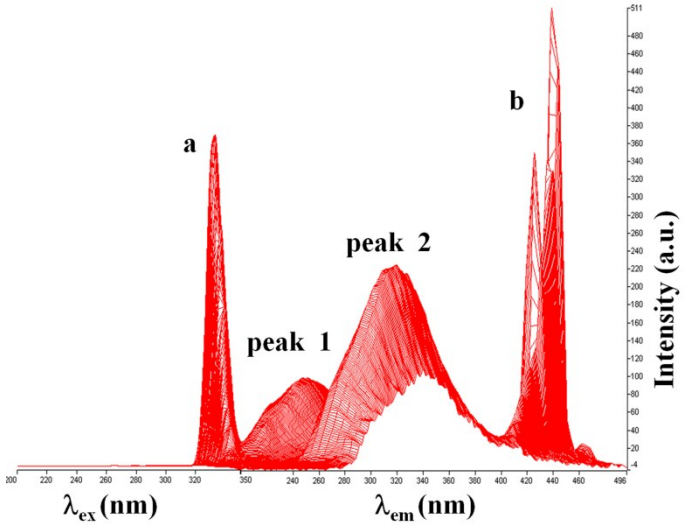

(a)

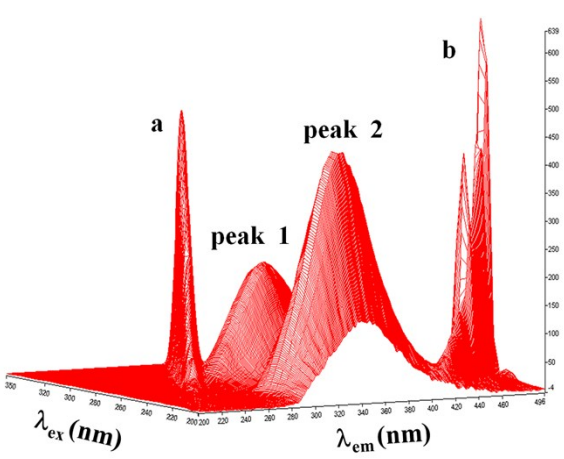

(b)

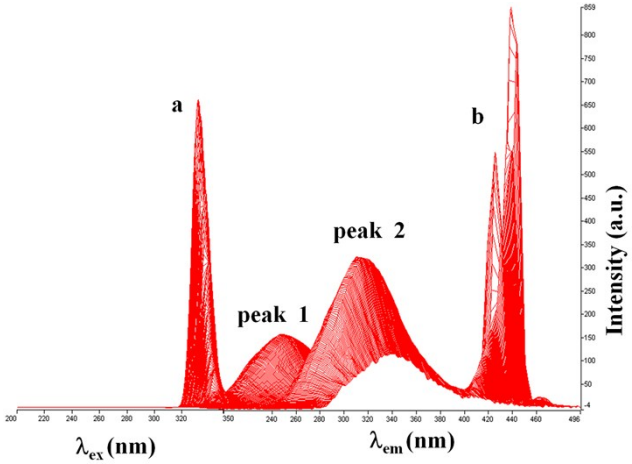

(c)

Fig. S17 The 3D fluorescence spectra of BSA + **1** (a), BSA + **2** (b), BSA + **4** (c). *c*(BSA) = 2 × 10^{-6} molL^{-1}, *c*(**1, 2** and **4**) = 2 × 10^{-6} molL^{-1}.

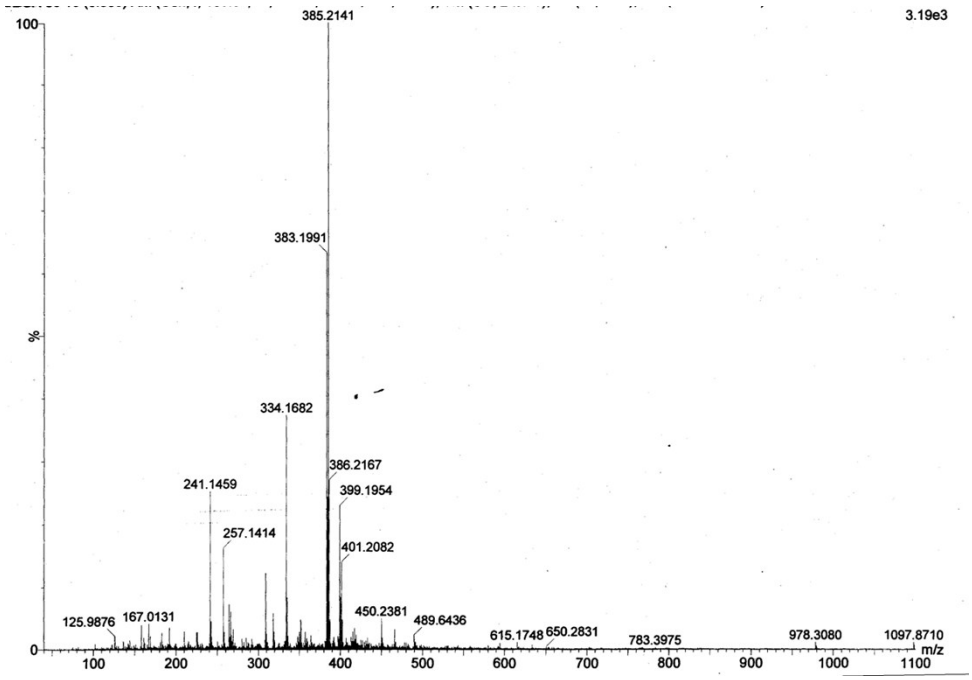

Fig. S18 ESI-MS spectra of **pmpzdpmH**.

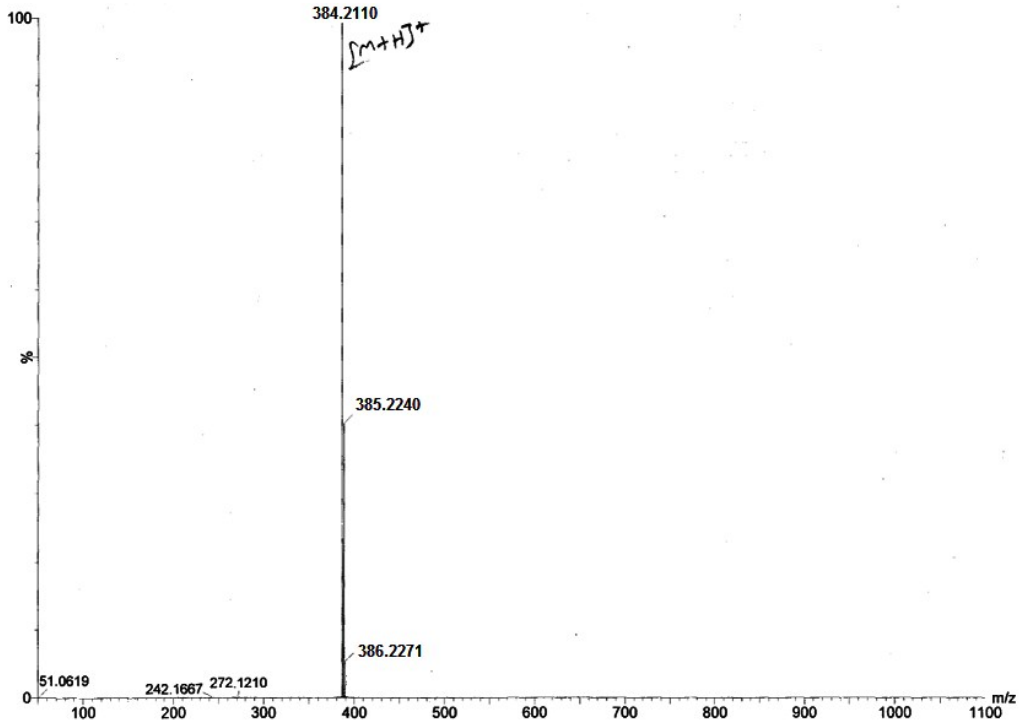

Fig. S19 ESI-MS spectra of **pypzdpmH**.

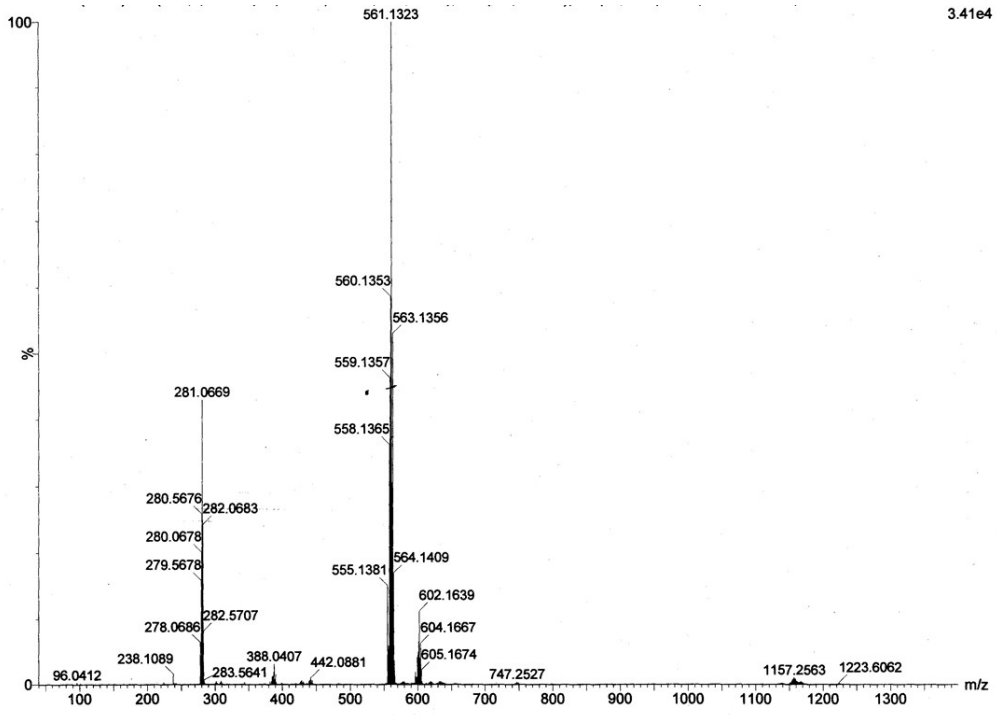

Fig. S20 ESI-MS spectra of **1**.

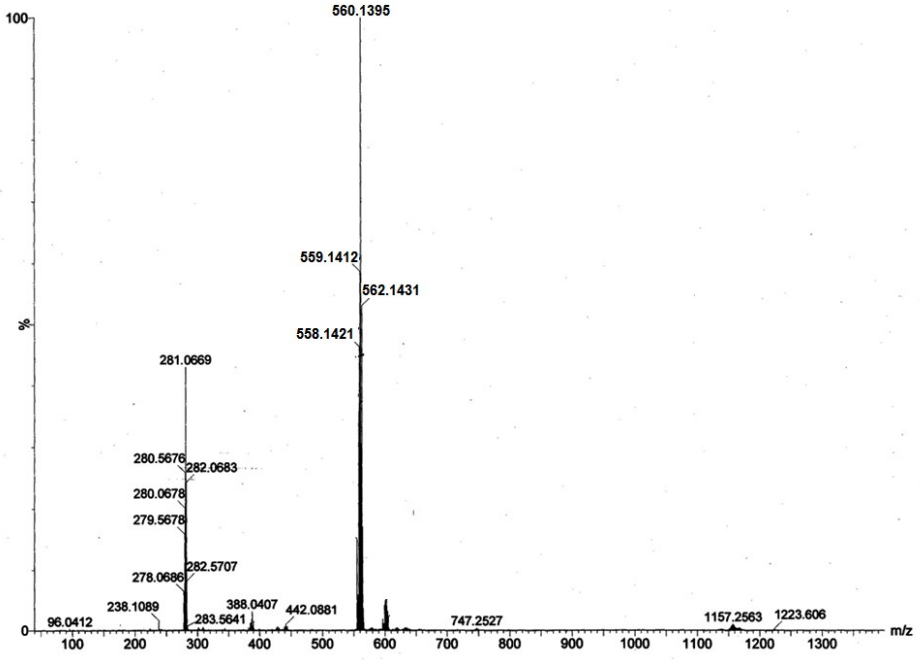

Fig. S21 ESI-MS spectra of **2**.

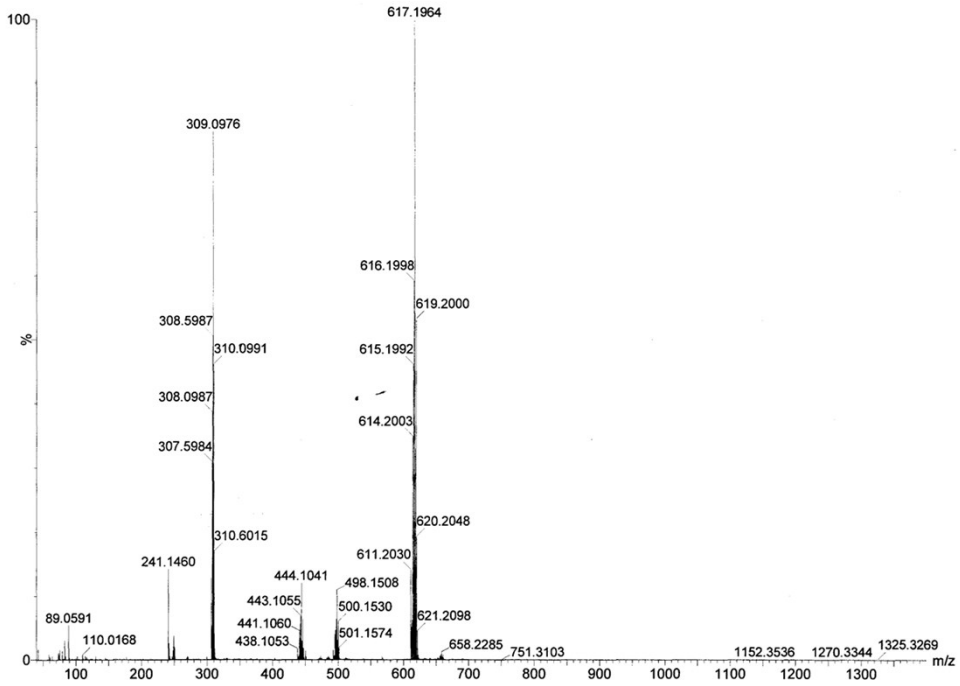

Fig. S22 ESI-MS spectra of **3**.

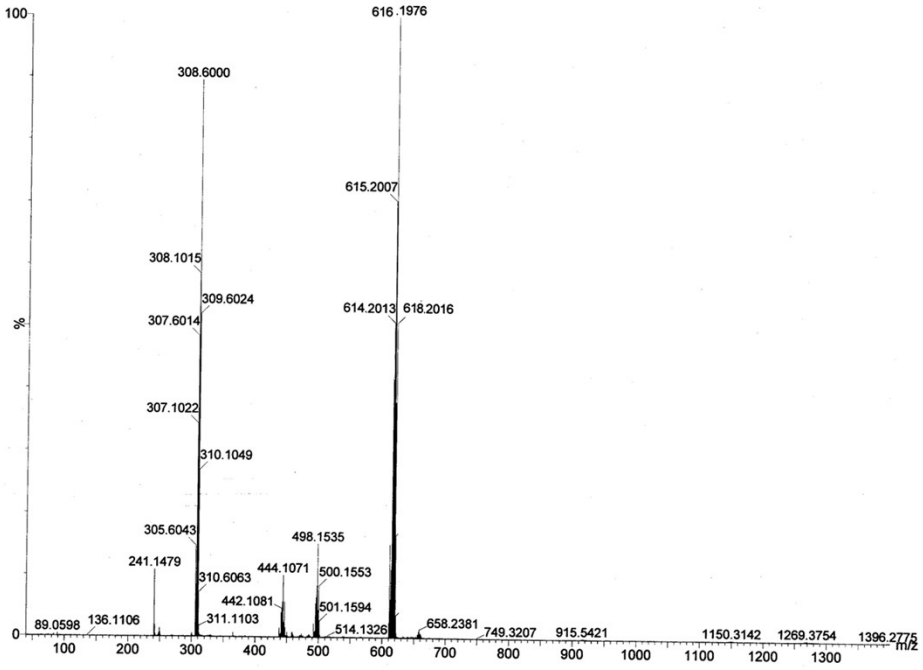

Fig. S23 ESI-MS spectra of **4**.

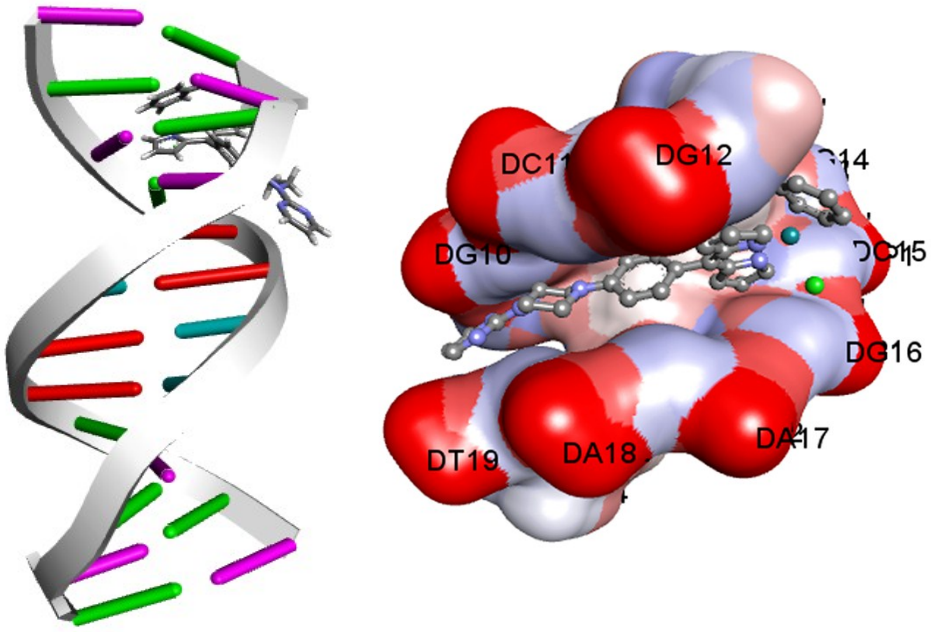

Fig. S24 Molecular docked model of complex **1** with DNA (PDB ID: 1BNA).

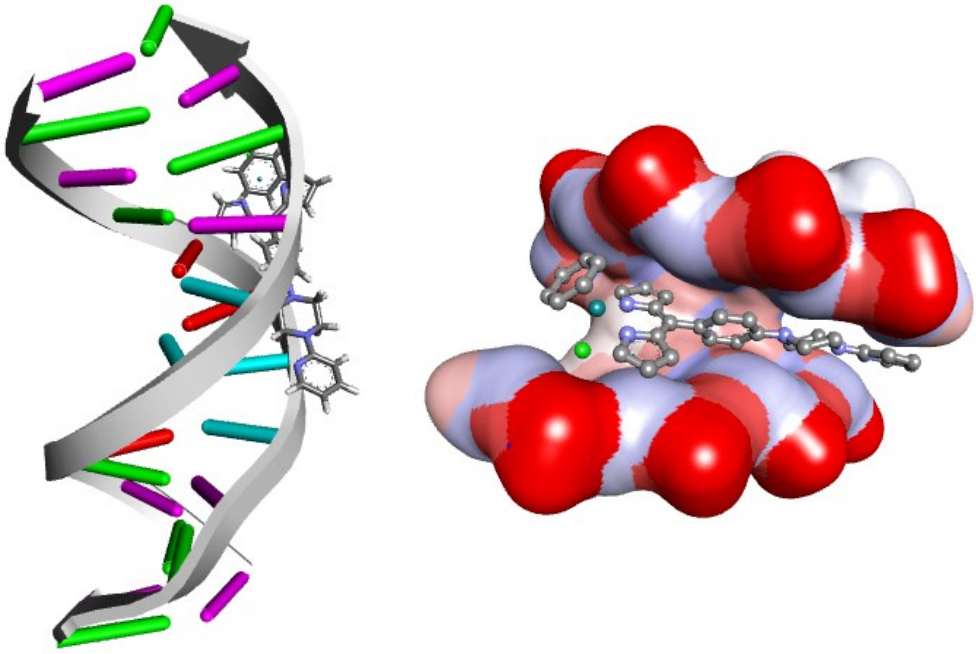

Fig. S25 Molecular docked model of complex **2** with DNA (PDB ID: 1BNA).

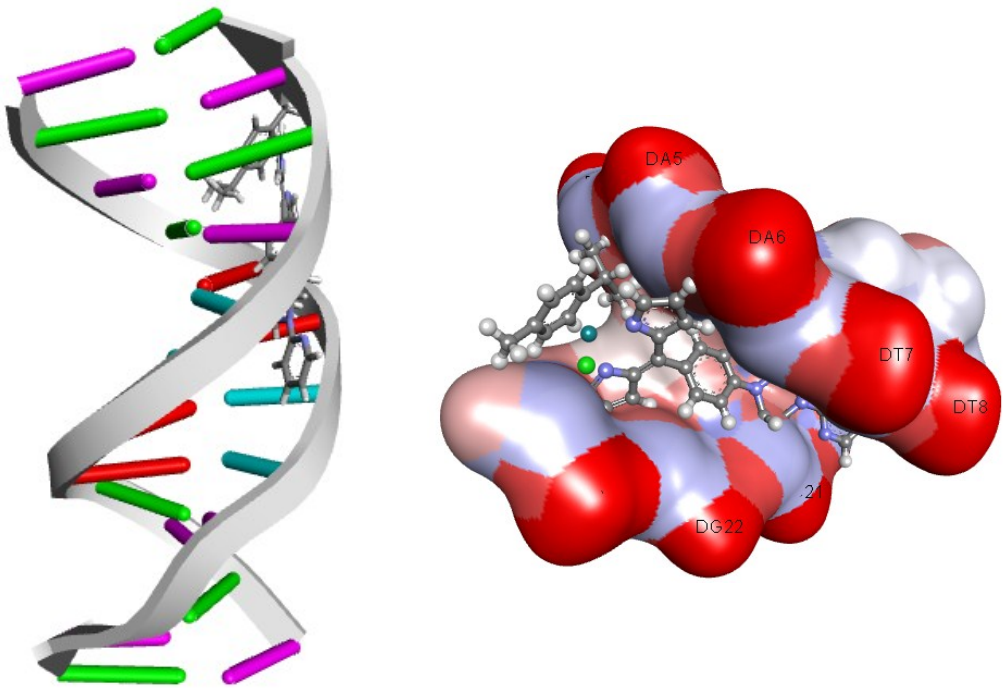

Fig. S26 Molecular docked model of complex **4** with DNA (PDB ID: 1BNA).

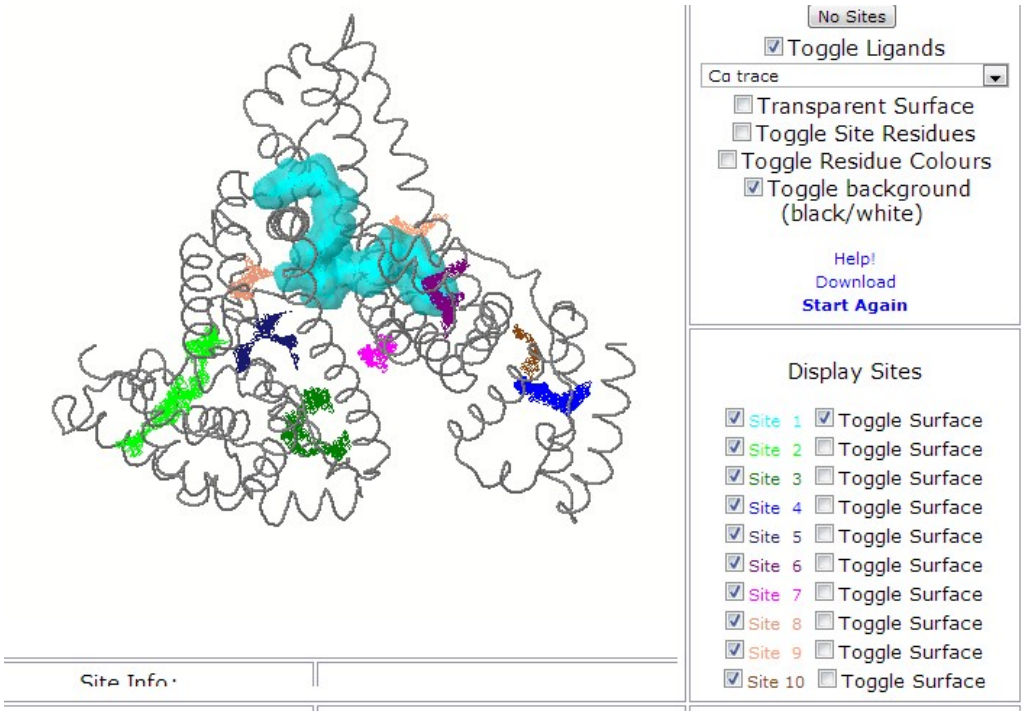

Fig. S27 Most probable 10 (ten) binding sites of HSA (PDBID: 1h9z).

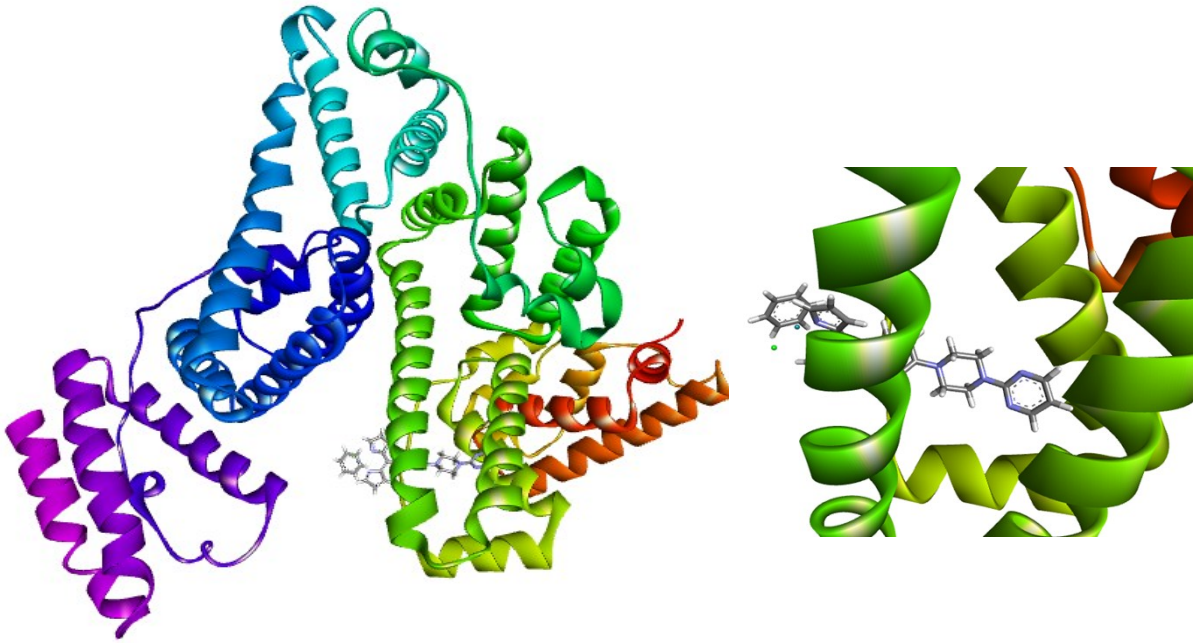

(a) (b)

Fig. S28 Molecular docked model of **1** located within the hydrophobic pocket of HSA (a) (PDB ID: 1h9z) (b) the interaction mode between **1** (stick) and HSA (cartoon).

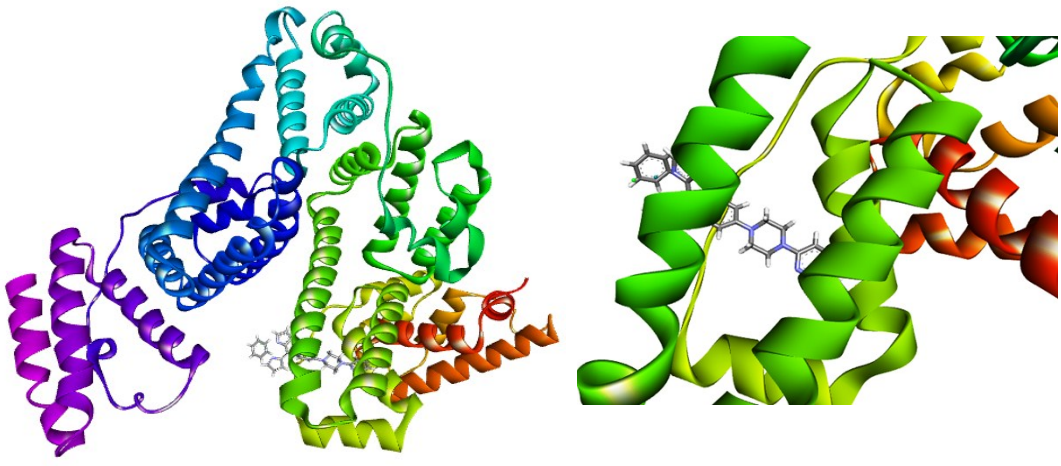

(a) (b)

Fig. S29 Molecular docked model of **2** located within the hydrophobic pocket of HSA (a) (PDB ID: 1h9z) (b) the interaction mode between **2** (stick) and HSA (cartoon).

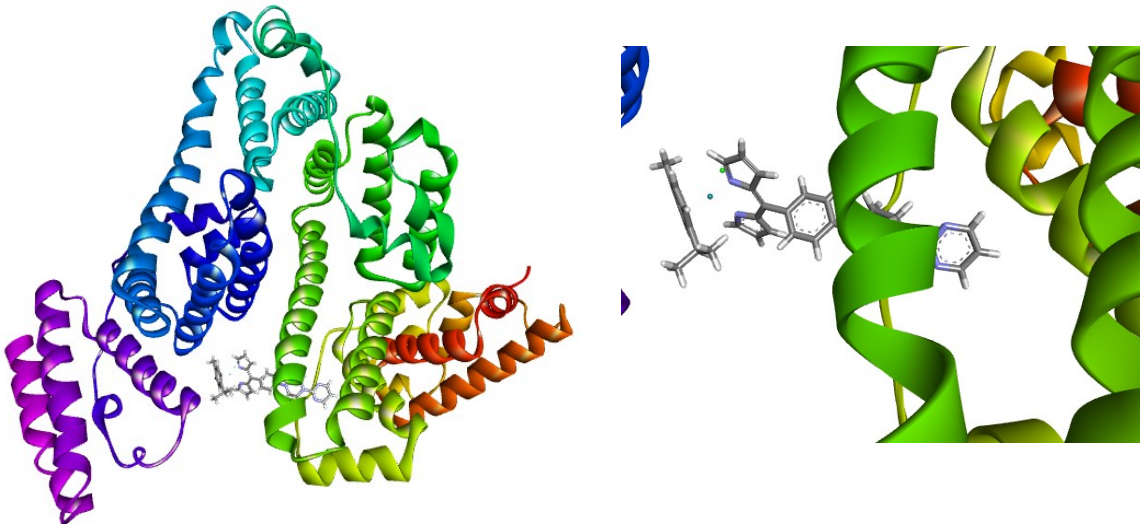

(a) (b)

Fig. S30 Molecular docked model of **4** located within the hydrophobic pocket of HSA (a) (PDB ID: 1h9z) (b) the interaction mode between **4** (stick) and HSA (cartoon).

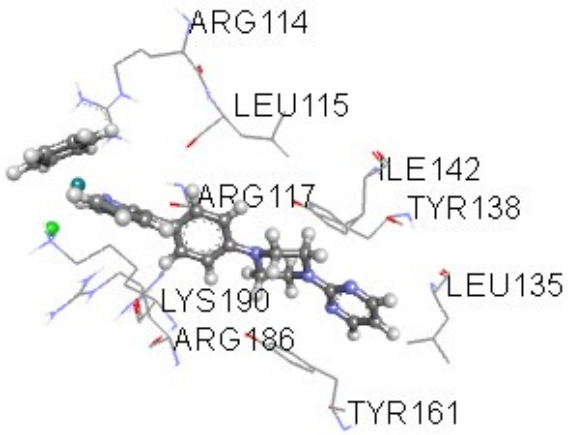

Fig. S31 Interaction of complex **1** with HSA subdomain IIA.

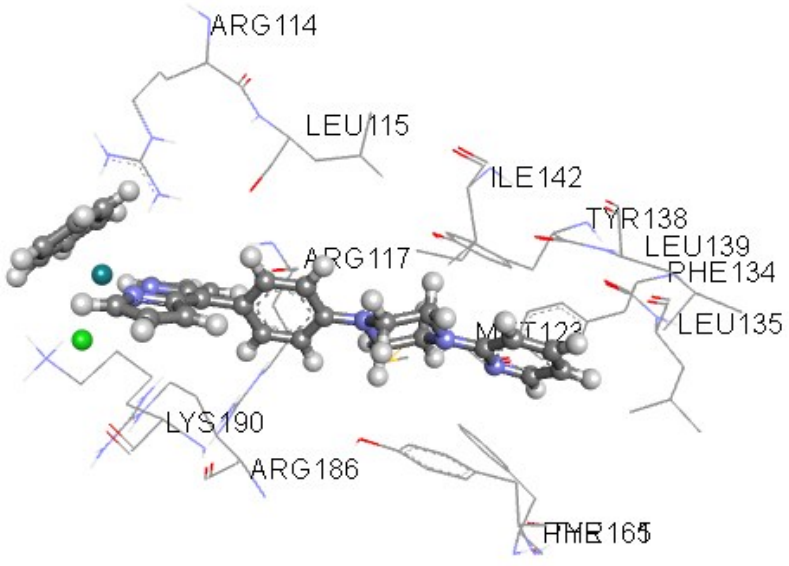

Fig. S32 Interaction of complex **2** with HSA subdomain IIA.

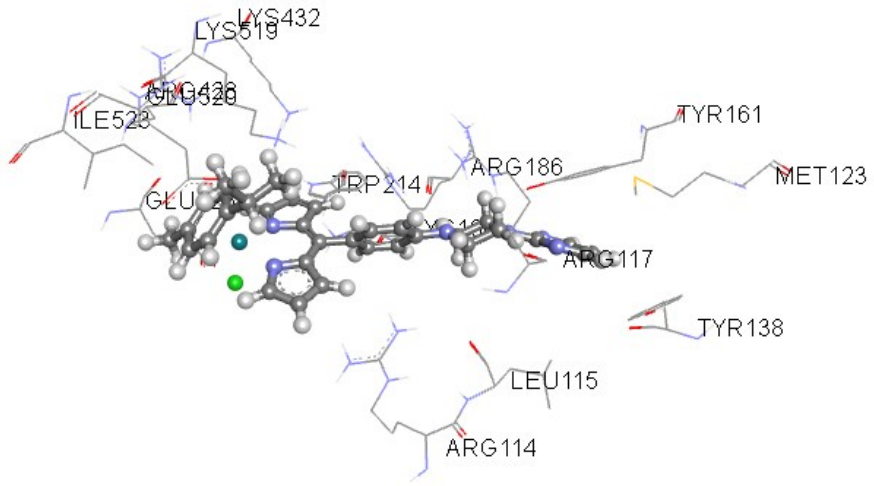

Fig. S33 Interaction of complex **3** with HSA subdomain IIA.

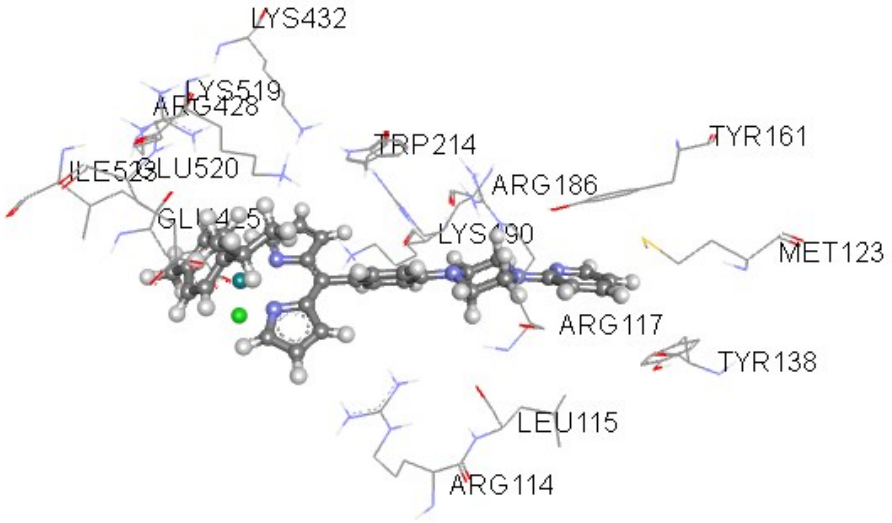

Fig. S34 Interaction of complex **4** with HSA subdomain IIA.

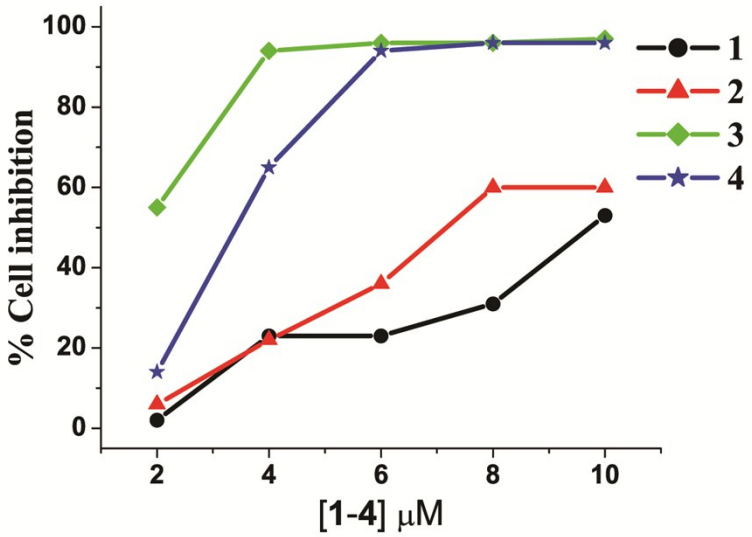

Fig. S35 MTT assay: Cells were treated with 2.0, 4.0, 6.0, 8.0 and 10.0 μM of **1**–**4** and percentage cell death plotted against different concentration of **1**–**4**.

Table S1

Bond length (Å)	**1**	**2**	**3**	**4**
Ru-N1	2.074	2.074	2.076	2.07
Ru-N2	2.080	2.081	2.086	2.08
Ru-Cl1	2.424	2.423	2.434	2.40
Ru-C*g*	1.775	1.776	1.773	1.774
Ru-C*av*	2.272	2.275	2.276	2.278
Bond Angle (˚)				
N2-Ru1-N1	92.58	92.58	92.58	92.58
N2-Ru1-Cl1	91.53	91.53	91.53	91.53
N1-Ru1-Cl1	90.32	90.32	90.32	90.32
ω	69.70	69.70	69.70	69.70

Selected bond lengths (Å) and bond angles (˚) from DFT calculated structure of **1**–**4**.

Table S2 HOMO and LUMO energy for complexes **1**–**4** calculated by DFT method.

Complexes	HOMO (ev)	LUMO (ev)
1	–5.130	–1.924
2	–5.142	–1.932
3	–5.073	–1.862
4	–5.066	–1.852

Table S3

Absorption Spectral Properties of 1–4 Bound to CT DNA.

Complexes	λ_{max} (nm)	Changes in absorbance	$\Delta\varepsilon$ $M^{-1}cm^{-1}$	Red/blue shift (nm)	K_b (M^{-1})	Site Size (s)
1	249	hyperchromism	0.428	2	9.5×10^4	0.14
	427	hypochromism	0.020	Insignificant		
	489	hypochromism	0.04	2		
2	248	hyperchromism	0.608	2	7.6×10^4	0.15
	425	hypochromism	0.010	Insignificant		
	490	hypochromism	0.030	2		
3	250	hyperchromism	0.370	4	6.9×10^5	0.15
	422	hypochromism	0.028	Insignificant		
	488	hyperchromism	0.069	2		
4	250	hyperchromism	0.362	4	6.5×10^5	0.15
	422	hypochromism	0.021	Insignificant		
	488	Hypochromism	0.063	2		

Complexes	Temperature (K)	K_q (M^{-1})	K_{bin} (M^{-1})	n	R

Table S4 Quenching constant (K_q), binding constant (K_{bin}) and number of binding sites (n) for the interactions of complexes with BSA

1	298	1.94×10^4	2.49×10^4	0.95	0.9984
	308	1.23×10^4	2.12×10^4		0.9987
2	298	3.32×10^4	4.49×10^4	0.97	0.9989
	308	3.02×10^4	4.31×10^4		0.9969
3	298	6.45×10^5	9.23×10^5	1.01	0.9991
	308	6.21×10^5	9.02×10^5		0.9989
4	298	2.30×10^5	4.43×10^5	1.02	0.9983
	308	2.15×10^5	4.29×10^5		0.9989

Table S5. Characteristic 3D fluorescence spectral parameters of the BSA and BSA + **1**–**4**

Complex	Peaks

	Rayleigh Peaks [$\lambda_{ex}/\lambda_{em}$ (nm/nm)]	Peak 1 [$\lambda_{ex}/\lambda_{em}$ (nm/nm)]	Intensity	Peak 2 [$\lambda_{ex}/\lambda_{em}$ (nm/nm)]	Intensity
BSA	270/270 → 350/350	280/340	264	223/342	653
1	270/270 → 350/350	280/340	102	221/340	304
2	270/270 → 350/350	280/340	126	221/340	397
3	270/270 → 350/350	280/340	80	221/340	214
4	270/270 → 350/350	280/340	95	221/340	275

Table S6 Log *P* Values for Complexes **1-4**[a]

Log *P*

Complex	Mean	SD
1	1.26	0.02
SITE 1	LYS 195, GLN 196, LEU 198, LYS 199, SER 202, LEU 203, PHE 206, GLY 207, GLU 208, ARG 209, ARG 209, ALA 210, PHE 211, LYS 212, ALA 213, TRP	
2	1.23	0.02
3	1.32	0.01
4	1.30	0.02
[a] Results are the means of three independent experiments and are expressed as means ± SDs.		

Table S7 5 most probable binding sites of HSA (PDB ID: 1h9z; Q-site finder) and preferential binding site of complexes from docked structure.

	214, VAL 216, ARG 218, GLN 221, VAL 235, HIS 242, ASN 295 LYS 323, ASP 324, LEU 327, GLY 328, LEU 331, PRO 339, TYR 341, SER 342, VAL 343, VAL 344, LEU 345, LEU 346, LEU 347, ARG 348, ALA 350, LYS 351, GLU 354, GLU 383, Pro 384, LEU 397, ILE 388, LYS 389, ASN 391, CYS 392, PHE 395, PHE 403, LEU 407, ARG 410, TYR 411, LEU 430, GLY 431, Val 433, GLY 434, CYS 437, CYS 438, ARG 445, MET 446, PRO 447, CYS 448, ALA 449, GLU 450, ASP 451, LEU 453, SER 454, VAl 455, LEU 457, VAL 455, LEU 457, ASN 458, SER 480, LEU 481, VAL 482, ARG 484, ARG 485, PRO 486, SER 489
SITE 2	VAL 7, ARG 10, LEU 14, PHE 19, LEU 22, VAL 23, ALA 26, PHE 27, TYR 30, GLU 45, VAL 46, PHE 49 ASN 61, LEU 66, HIS 67, THR 68, LEU 69, PHE 70, ASP 72, LYS 73, THR 76, ASN 99, LRU 103, TYR 150, ALA 151, PRO 152, GLY 248, ASP 249, LEU 250, LEU 251, ALA 254, ASP 255, ARG 257, ALA 258, ALA 261, LEU 283, LEU 284, GLU 285, LYS 286, SER 287, HIS 288
SITE 3	LEU 115, VAL 116, ARG 117, PRO 118, MET 123, PHE 134, LEU 135, TYR 138, LEU 139, ILE 142, HIS 146, PHE 149, LEU 154, PHE 157, ALA 158, TYR 161, LYS 162, PHE 165, LEU 182, ASP 183, LEU 185, ARG 186, GLY 189, LYS 190, SER 193
SITE 4	TYR 401, ASN 405, PHE 502, PHE 507, PHE 509, LYS 524, LYS 525, GLN 526, ALA 528, LEU 529, LEU 532, HIS 535, LYS 536, VAL 547, MET 548, PHE 551, ALA 552, LEU 575, VAL 576, SER 579, GLN 580
SITE 5	GLN 29, LYS 106, ASP 108, HIS 146, PRO 147, TYR 148, PHE 149, TYR 150, ALA 151, GLU 153, SER 192, SER 193, ALA 194, LYS 195, GLN 196, ARG 197, LYS 199, CYS 200, ALA 201, HIS 242, GLU 244, CYS 245, CYS 246, HIS 247, GLY 248, ASP 249, LEU 250, CYS 253, ARG 257
1	ARG 114, LEU 115, ARG 117, LEU 135, TYR 138, ILE 142, TYR 161, PHE 165, ARG 186, LYS 190
2	ARG 114, LEU 115, ARG 117, LEU 135, TYR 138, ILE 142, TYR 161, PHE 165, ARG 186, LYS 190

3	ARG 114, LEU 115, ARG 117, MET 123, TYR 138, TYR 161, ARG 186, LYS 190, TRP 214, GLU 425, ARG 428, LYS 432, LYS 479, GLU 520, ILE 523
4	ARG 114, LEU 115, ARG 117, MET 123, TYR 138, TYR 161, ARG 186, LYS 190, TRP 214, GLU 425, ARG 428, LYS 432, LYS 479, GLU 520, ILE 523